JOURNAL OF GENERAL VIROLOGY

RESEARCH ARTICLE

Athukorala *et al.*, *Journal of General Virology* 2024;105:001928
DOI 10.1099/jgv.0.001928

MICROBIOLOGY SOCIETY

OPEN ACCESS

Structural and functional characterization of siadenovirus core protein VII nuclear localization demonstrates the existence of multiple nuclear transport pathways

Ajani Athukorala[1], Camilla M. Donnelly[2], Silvia Pavan[3], Sepehr Nematollahzadeh[3], Victoria Atalie Djossou[3], Babu Nath[2], Karla J. Helbig[1], Enzo Di Iorio[3], Brian P. McSharry[2], Gualtiero Alvisi[3], Jade K. Forwood[2] and Subir Sarker[1,4,*]

Abstract

Adenovirus protein VII (pVII) plays a crucial role in the nuclear localization of genomic DNA following viral infection and contains nuclear localization signal (NLS) sequences for the importin (IMP)-mediated nuclear import pathway. However, functional analysis of pVII in adenoviruses to date has failed to fully determine the underlying mechanisms responsible for nuclear import of pVII. Therefore, in the present study, we extended our analysis by examining the nuclear trafficking of adenovirus pVII from a non-human species, psittacine siadenovirus F (PsSiAdV). We identified a putative classical (c)NLS at pVII residues 120–128 (^{120}PGGFKRRRL^{128}). Fluorescence polarization and electrophoretic mobility shift assays demonstrated direct, high-affinity interaction with both IMPα2 and IMPα3 but not IMPβ. Structural analysis of the pVII-NLS/IMPα2 complex confirmed a classical interaction, with the major binding site of IMPα occupied by K^{124} of pVII-NLS. Quantitative confocal laser scanning microscopy showed that PsSiAdV pVII-NLS can confer IMPα/β-dependent nuclear localization to GFP. PsSiAdV pVII also localized in the nucleus when expressed in the absence of other viral proteins. Importantly, in contrast to what has been reported for HAdV pVII, PsSiAdV pVII does not localize to the nucleolus. In addition, our study demonstrated that inhibition of the IMPα/β nuclear import pathway did not prevent PsSiAdV pVII nuclear targeting, indicating the existence of alternative pathways for nuclear localization, similar to what has been previously shown for human adenovirus pVII. Further examination of other potential NLS signals, characterization of alternative nuclear import pathways, and investigation of pVII nuclear targeting across different adenovirus species is recommended to fully elucidate the role of varying nuclear import pathways in the nuclear localization of pVII.

INTRODUCTION

Adenoviruses are complex DNA viruses identified in all types of vertebrates causing both clinical and subclinical infections [1–3]. Human adenoviruses are the most extensively studied and are usually associated with respiratory, gastrointestinal and ocular infections [2]; the next most studied adenoviruses are from domestic and wild avian species [1, 4]. The capsid structure of adenoviruses comprises three primary capsid proteins, namely hexon, penton and fibre, along with several major and minor core proteins that aid in assembling and maintaining the viral core [2, 3].

The core of the adenovirus virion has three major proteins, pV, pVII and adenovirus terminal protein, with protein VII (pVII) being the most abundant. pVII is a highly basic, arginine-rich, functional analogue of histones that condenses dsDNA by wrapping it around the protein [2, 3]. Mature pVII is derived from a precursor protein (pre-pVII) by proteolytic processing.

Received 04 August 2023; Accepted 21 November 2023; Published 23 January 2024
Author affiliations: [1]Department of Microbiology, Anatomy, Physiology, and Pharmacology, School of Agriculture, Biomedicine and Environment, La Trobe University, Melbourne, VIC 3086, Australia; [2]School of Dentistry and Medical Sciences, Biomedical Sciences, Charles Sturt University, Wagga Wagga, NSW, Australia; [3]Department of Molecular Medicine, University of Padua, Via Gabelli 63, 35121 Padua, Italy; [4]Biomedical Sciences & Molecular Biology, College of Public Health Medical, and Veterinary Sciences, James Cook University, Townsville, QLD 4811, Australia.
***Correspondence:** Subir Sarker, subir.sarker@jcu.edu.au;s.sarker@latrobe.edu.au
Keywords: adenovirus protein VII; importin α/β-mediated nuclear import; nuclear localization; psittacine siadenovirus F.
Abbreviations: CLSM, confocal laser scanning microscopy; EMSA, electrophoretic mobility shift assay; FPLC, fast protein liquid chromatography; HAdV, human adenovirus; His-Tag, poly histidine-tag; IMP, importin; MX2, high-flux undulator microfocus beamline; NLS, nuclear localization signal; PDB, protein data bank; PsSiAdV, psittacine siadenovirus F; pVII, protein VII; TEV, tobacco etch virus.
Protein Data Bank accession code: 8SV0.
Two supplementary tables and one supplementary figure is available with the online version of this article.

Impact Statement

The impact of circulating adenoviruses on the critically endangered orange-bellied parrot (OBP) population could be devastating, considering the OBP already faces numerous threats to its survival in the wild. Conservation of the OBP population is also heavily reliant on a better understanding of infecting pathogens. This study, using a predicted classical nuclear localization signal sequence in protein VII of psittacine siadenovirus F (PsSiAdV), highlights its ability to mediate high-affinity binding to IMPα, leading to IMPα/*β*-dependent nuclear targeting. Further, its ability to localize to the nucleus, despite IMPα/*β* pathway inhibition, highlights PsSiAdV pVII's capacity to utilize multiple nuclear import pathways. These results advance our understanding of the diverse mechanisms governing adenovirus nuclear import, which may help to develop future antiviral therapeutics for the conservation of the endangered OBP.

Both pre-pVII and mature pVII appear to be essential for nuclear localization of the adenovirus genome during viral infection [5–8] but the mechanism of adenovirus pVII nuclear entry remains to be fully defined. In addition, pVII plays important roles in regulating host response pathways such as inflammatory signalling and the DNA damage response, during adenoviral infection in humans [9–12], with these functions of pVII appearing to be dependent on its nuclear localization.

Nuclear localization signals (NLSs) are short signal sequences that mediate the nuclear transport of proteins facilitating the passage of cargo molecules through the nuclear envelope [13]. Several early studies identified multiple predicted NLSs in pVII of species C human adenovirus (HAdV), for example HAdV-C5 and HAdV-C2 [6–8] which interact with several different cellular transporters, including importin (IMP) α/*β*, IMP*β*, transportin and IMP7. Therefore, HAdV pVII is believed to be imported into the nucleus by multiple active nuclear transport mechanisms [6–8]. Moreover, it has been suggested that NLS regions on pVII, which bind to various IMPs, play a key role in maintaining the solubility of the protein following disintegration of the capsid. Additionally, NLS activity is particularly important during the late stages of viral replication, ensuring the nuclear accumulation of pVII and thereby contributing to the overall success of viral replication [8, 14].

Previous studies have mainly focused on HAdVs. However, pVII homologues have been identified in all adenoviruses studied to date, with variations between pVII sequences in adenoviruses from different species being identified [7]. To expand our knowledge on the nuclear import of pVII this study sought to examine an avian homologue of HAdV-C pVII in a recently described adenovirus, the psittacine siadenovirus F, identified from one of the most critically endangered Australian parrots, the orange-bellied parrot (*Neophema chrysogaster*) [15]. In this study, we aimed to elucidate the structural and functional properties of the predicted NLS of psittacine siadenovirus F (PsSiAdV) pre-pVII, and to better understand the mechanisms underlying its nuclear transport using a combination of structural biology, biochemical and imaging techniques. We identified a classical (c)NLS in pre-pVII of PsSiAdV (residues 120–128) capable of mediating high-affinity binding to the IMPα major binding site and conferring IMPα/*β*-dependent nuclear targeting properties to heterologous proteins. We show that a GFP-pVII fusion protein could localize to the cell nucleus, despite inhibition of the IMPα/*β* pathway, implying that PsSiAdV has the capacity to utilize multiple nuclear import pathways. We also report that pre-pVII does not accumulate in the nucleolus, in contrast to what has been reported for HAdV-C2 [7].

METHODS

Peptide and gene construct design and synthesis

The adenovirus pVII sequence of psittacine siadenovirus F [15] was identied through GenBank (Accession number. MW365934) and potential NLSl sequences were analysed by the cNLS mapper program [16]. A monopartite NLS with a score of 11.0 for residues 120–128 was predicted (^{120}PGGFKRRRL^{128}). A synthetic peptide corresponding to the predicted amino acid residues along with an FITC tag and Ahx sequence at the N-terminus, referred to herein as PsSiAdV pVII-NLS, was obtained from GenScript.

N-terminally truncated IMPα2 and IMPα3 isoforms lacking the autoinhibitory importin *β* binding IBB domain (mouse IMPα2: mIMPα2ΔIBB; His tag, TEV site, and human importin α3: hIMPα3ΔIBB; His tag, TEV site), and IMP*β* encoded by the pET30a expression vector have been described previously [17, 18].

Recombinant protein expression and purification

Overexpression of IMPs was performed in *Escherichia coli* pLysS cells via the auto-induction method [19]. After induction, cultures were centrifuged at 6000 r.p.m. for 20 min at 4°C and isolated bacterial pellets were resuspended in HIS buffer A (50 mM phosphate buffer, 300 mM NaCl, 20 mM imidazole, pH 8). Cells were lysed through two freeze–thaw cycles. Lysozyme (Sigma-Aldrich; 1 ml of 20 mg ml^{-1}) and DNase (Sigma-Aldrich; 10 µl of 50 mg ml^{-1}) were then added and incubated at room temperature for 1 h. Supernatants were collected via centrifugation at 12000 r.p.m. for 30 min at 4°C. Soluble extracts

were filtered through 0.45 µm low-protein affinity filters and subsequently injected onto a 5 ml HisTrap HP column (GE Healthcare), which had been pre-equilibrated with His buffer A, in an AKTA purifier fast protein LC device (GE Healthcare). Following washing with 20 column volumes of His buffer A, proteins were eluted via a gradually increasing gradient of imidazole (20 to 500 mM; ChemSupply). Eluted protein fractions were pooled and loaded into a pre-equilibrated HiLoad 26/60 Superdex 200 column (GE Healthcare) in GST buffer A (50 mM Tris, 125 mM NaCl) for further purification employing size-exclusion chromatography. Eluted volumes at corresponding protein sizes were collected and concentrated via an Amicon MWCO 10 kDa filter (Merck Millipore). Samples were assessed for purity by SDS-PAGE by running protein samples at 165 V for 30 min on a 4–12% Bis-Tris plus gel (Thermo Fisher Scientific) prior to experimental use.

Crystallization, data collection and structure determination

For IMPα2, PsSiAdV pVII-NLS was crystallized by the hanging drop vapour diffusion method. The protein complex was obtained at a 1:1 ratio in a 300 µl reservoir of 600 mM sodium citrate (pH 6.5) and 10 mM DTT at 23°C. Individual rod-shaped crystals were formed within 2 days of incubation. Collected crystals were cryoprotected in the reservoir solution containing 20% glycerol, before being flash frozen in liquid nitrogen.

X-ray diffraction data were obtained from the Australian Synchrotron on the MX2 macromolecular beam lines [20] using the Eiger 16 M detector. Data were indexed and integrated using MOSFLM [21]. Merging, space group assignment, scaling and R_{free} calculations were performed using AIMLESS within CCP4 [22]. Final model building and refinement were performed using iterative cycles of COOT [23] and Phenix [24]. Phasing was performed using molecular replacement in Phaser [25] and PDB code 1IQ1 was used as the search model for IMPα2. The finalized model was validated and deposited with the PDB (8SV0) as detailed in Table S1 (available in the online version of this article).

Electrophoretic mobility shift assays

FITC-labelled PsSiAdV pVII-NLS synthetic peptide was mixed with 20 µM of IMP isoforms in a 1:1 ratio to a total volume of 17 µl. Mixtures were incubated for 15 min at room temperature and then supplemented with 3 µl of 50% glycerol. Samples were run on a 1% agarose TB gel (3 mM Tris, 1 mM boric acid, 1% agarose, pH 8.5) for 1.5 h at 70 V in TB running buffer (3 mM Tris, 1 mM boric acid, pH 8.5). The images were initially captured using an SYBR green filter using the BioRad Gel Doc imaging system and then stained using Coomassie stain. Gels were destained with 10% ethanol and 10% glacial acetic acid overnight and images were captured using the BioRad Gel Doc imaging system.

Fluorescence polarization assays

FITC-tagged PsSiAdV pVII-NLS (5 nM) was incubated with two-fold serially diluted IMPs. IMPα isoforms (2 and 3) and IMP*β* were tested separately using a starting concentration as low as 5 nM, across 23 wells in 96-well black Fluotrac microplates (Greiner Bio-One), each containing an appropriate negative control (no IMP binding partner). The total volume was made up to 200µl per well with GST buffer A (50 mM Tris, 125 mM NaCl). Fluorescence polarization measurements were recorded immediately using a CLARIOstar Plus plate reader (BMG Labtech) and assays were performed in triplicate. Data from the three independent experiments were analysed using GraphPad Prism (Prism 9, v9.3.1) and used to determine the dissociation constant (K_d).

Cell culture and transfections

Plasmids

Plasmid pcDNA3.1-NT-GFP-TOPO, mediating the expression of GFP cycle3, and pcDNA3.1-NT-GFP-TOPO-SV40-NLS, mediating the expression of a fusion protein between GFP cycle3 and Simian vacuolating virus (SV) 40 large tumour antigen NLS (PKKKRKV-132), were described previously [26]. Plasmids pEGFP-N1-H1E and pEPI-GFP-human cytomegalovirus (HCMV)-UL44, encoding control GFP fusion proteins localizing to the nucleus via different IMPα/*β*-independent and IMPα/*β*-dependent pathways, respectively were described previously [27–29]. Plasmid DsRed-RanQ69L, encoding a *trans*-dominant negative, GTPasedeficient mutant of the Ran GTPase, which impairs Ran-dependent nuclear transport [30], was a generous gift from Michael Green (University of Massachusetts, USA). Plasmid mCherry-Bimax2, coding for a competitive inhibitor of the IMPα/*β* nuclear import pathway [31], was a generous gift from Yoshihiro Yoneda and Masahiro Oka (Osaka University, Japan). Plasmid pDsRed-C1-Fibrillarin [32], was kindly provided by Denis Archambault (University of Québec, Canada). Plasmids pEGFP-C1-HAdV-C2-pVII, pEGFP-C1-PsSiAdV-pVII and pEGFP-C1-PsSiAdV-pVII (120–128), mediating the expression of the respective GFP fusion proteins, were synthesized by BioFab research. A list of all plasmids used in this study is available in Table S2.

Cells

HEK293A cells were maintained in Dulbecco's modified Eagle's medium (DMEM) supplemented with 10% (v/v) FBS, 50 U ml^{-1} penicillin, 50 U ml^{-1} streptomycin and 2 mM L-glutamine in a humidified incubator at 37°C in the presence of 5% CO_2 and passaged when confluent as described previously [33].

Transfections

HEK293A cells were seeded in a 24-well plate onto glass coverslips (5×10^4 cells per well). The next day, cells were transfected with appropriate amounts of expression constructs (range 5–250 ng), using Lipofectamine 2000 (ThermoFisher Scientific), following the manufacturer's recommendations and further incubated at 37°C and 5% CO_2 in complete medium as described previously [34], until being processed for confocal laser scanning microscopy (CLSM).

Confocal laser scanning microscopy and image analysis

For detection of fluorescent proteins, 24 h post-transfection cells were incubated for 30 min with DRAQ5 (#62 251, ThermoFisher Scientific; 1:5000 in DMEM with no phenol red), washed twice with 1 PHEM (60 mM PIPES, 25 mM HEPES, 10 mM EGTA and 4 mM $MgSO_4$) and fixed with 4% (v/v) paraformaldehyde for 10 min at room temperature (RT). Following three washes with 1× PBS, coverslips were mounted on glass slides with Fluoromount G (Southern Biotech). Subcellular localization of fusion proteins was analysed using a Nikon A1 confocal laser scanning microscope (Nikon) equipped with a 60× oil immersion objective [35]. Levels of nuclear accumulation of proteins of interest were determined using the FiJi public domain software (https://doi.org/10.1038/nmeth.2019) from single-cell measurements for each of the nuclear (Fn), nucleolar (Fnu) and cytoplasmic (Fc) fluorescence, after the subtraction of fluorescence due to autofluorescence/background as described previously [35, 36]. Nucleoli were identified as fibrillarin-positive areas, while DRAQ5 was used to identify cell nuclei and a small area between the cell boundary and the DRAQ5-positive region was used to measure the cytoplasmic signal. Data were statistically analysed by performing either a Student's t-test, or one-way or two-way ANOVA using GraphPad Prism 9 software (GraphPad).

Statistical analysis

Statistical analysis was conducted using different methods depending on the number of groups being compared. Student's t-tests were used for comparing two groups, while experiments involving two or more experimental groups were statistically analysed using either a one-way or two-way multiple comparison ANOVA, or multiple t-tests. A significance level of $P<0.05$ was considered statistically significant. Unless specified otherwise, all statistical analyses were performed using GraphPad Prism 9 software (GraphPad). The experiments were conducted in biological triplicates unless stated otherwise. The error bars represent the mean±SEM, and significance was denoted by a P value of <0.05. Asterisks were used to indicate significance levels: $*P<0.05$, $**P<0.01$, $***P<0.001$ and $****P<0.0001$.

RESULTS

Bioinformatic identification of cNLSs within PsSiAdV pVII compared with HAdV-C2 pVII

According to prior research [6–8], it is evident that the pVII protein of species C HAdV has multiple functional NLSs that allow it to be transported to the nucleus and the nucleolus of the host cell via different import pathways. In our study, we used HAdV-C2 as a reference to analyse the primary sequence of PsSiAdV pVII and detect potential NLSs [6–8]. Using the cNLS mapper online tool, our analysis found a highly probable monopartite NLS with a score of 11.0 at the C-terminus (residues 120–128:^{120}PGGFKRRRL^{128}) of PsSiAdV pVII (Fig. 1). However, pairwise alignment of amino acid sequences of the pVII gene from PsSiAdV [15] and HAdV-C2 [7, 8] revealed significant differences, with <26% amino acid sequence similarity (Fig. 1a). In addition, predicted NLS regions are not conserved. Thus, the study investigated whether the putative cNLS of pVII from an avian adenovirus, PsSiAdV, has the ability to mediate nuclear trafficking.

PsSiAdV pVII-NLS binds with high affinity to IMPα2 and IMPα3 but not to IMP*β*

The presence of a putative cNLS in the PsSiAdV pVII protein suggested an ability to be transported to the nucleus, as previously reported for pVII of HAdV [6–8]. To confirm this hypothesis we investigated the binding interactions between PsSiAdV pVII-NLS (residues 120–128) and IMPs. Initially, an electrophoretic mobility shift assay (EMSA) was used to assess FITC-tagged PsSiAdV pVII-NLS interactions with IMPα2, IMPα3 and IMP*β*. IMPs migrated toward the anode, whereas the FITC-tagged PsSiAdV pVII-NLS peptide migrated toward the cathode (Fig. 2a). However, in the presence of a corresponding binding partner, the bound IMP/FITC-tagged peptide was expected to shift the migration toward the anode, developing a distinct band. Upon incubation with either IMPα2 or α3, the FITC-labelled PsSiAdV pVII-NLS migrated differently, due to direct interaction with the recombinant proteins, as highlighted by the yellow colour in the merged Coomassie and UV images (Fig. 2a, bottom panel). However, IMP*β* mixed with the PsSiAdV pVII-NLS peptide appeared to have no interaction, resulting in the presence of two separate bands in a similar manner to the IMP-only and peptide-only samples. Therefore, our experimental results suggest that the PsSiAdV pVII-NLS peptide is capable of binding to IMPα (α2 and α3) but not IMP*β* (Fig. 2a), as expected from a bona fide cNLS.

To further evaluate the interaction and to determine the binding strength of the IMP/peptide complexes, quantitative fluorescence polarization assays were performed. As expected, analysis showed a high-affinity interaction between PsSiAdV pVII-NLS and

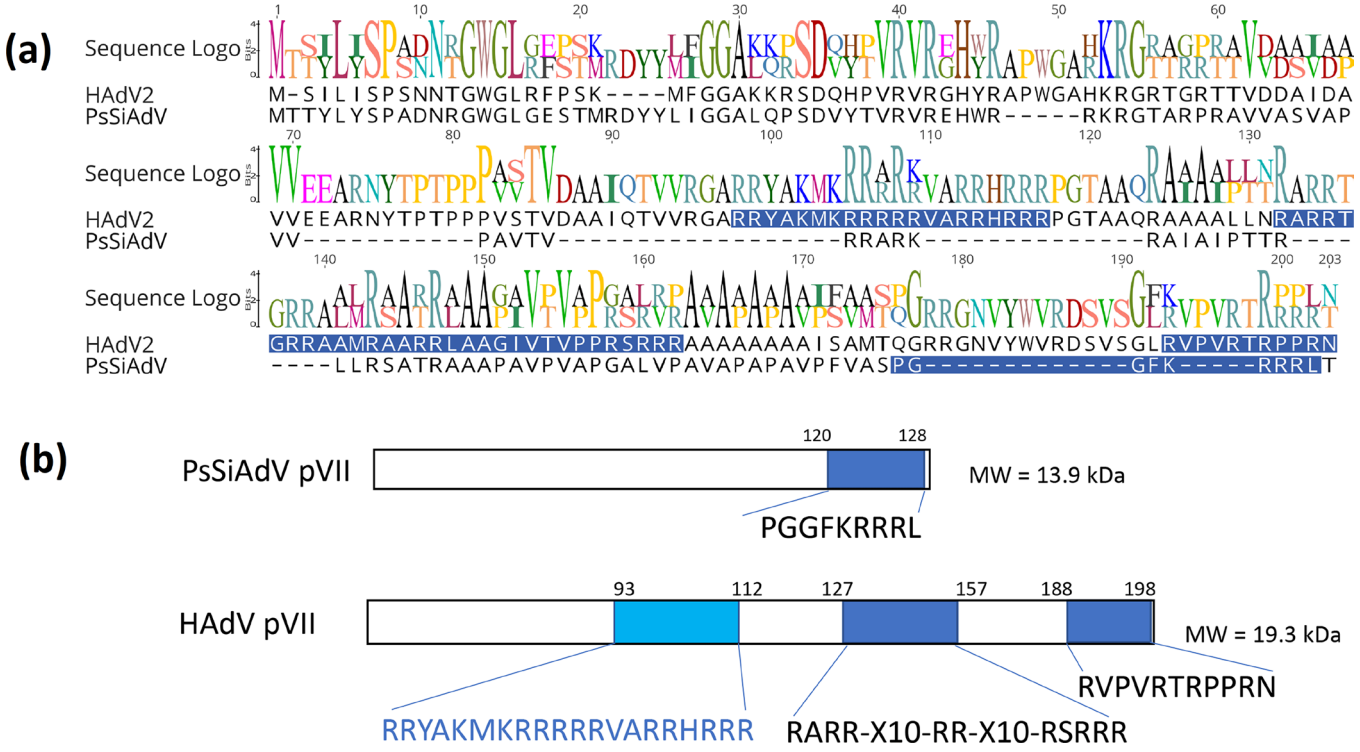

Fig. 1. Schematic illustration to exhibit the location of NLS regions in adenovirus pVII. (a) Sequences of pVII from psittacine siadenovirus F (PsSiAdV pVII) (GenBank Accession no.: MN687905.1) [15] and human adenovirus-C2 (HAdV pVII) (GenBank Accession no.: AC_000008) [7, 8] were aligned using Geneious Prime (v21.1.1, Biomatters). Previously described NLSs and nucleolar localization signal (NoLS) from HAdV-C2 and a putative NLS of PsSiAdV pVII are highlighted in blue shading [7, 8]. (b) Simplified diagram displaying the identified NLS and nucleolar localization (NoLS) regions.

IMPα isoforms at the nanomolar level (IMPα2, K_d 277.8 nM; IMPα3, K_d 892.3 nM) whereas IMPβ again displayed limited binding capacity (Fig. 2b).

The high-resolution crystal structure reveals the classical binding interface of IMPα2 and PsSiAdV pVII-NLS

To better understand how the PsSiAdV pVII might traffic to the nucleus, we crystallized the predicted NLS region in pVII (residues 120–128) in complex with the nuclear import protein IMPα2. Protein co-crystallization was performed using the hanging-drop method and large rod-shaped crystals formed (Fig. 3a) after 2 days of incubation. Crystals were diffracted at the Australian synchrotron on the MX2 beamline and the structure was solved to 2.2 Å resolution. Data were indexed in the space group P21 21 21 with the unit cell parameters $a = 77.22$, $b = 88.73$, $c = 96.41$. The structure was solved in Phaser [25] by molecular replacement with PDB 3UKX as the model. The structure contained one molecule of IMPα2ΔIBB and two chains of PsSiAdV pVII-NLS. The model was refined in Phenix [24], and modelling was performed in COOT [23, 24], with the final structure having good R_{work} and R_{free} of 22.9 and 24%, respectively. The full data collection and refinement statistics are given in Table S1.

The final model contained IMPα2ΔIBB (residues 72–498), with PsSiAdV pVII-NLS residues ^{120}PGGFKRRRL^{128} bound to the major binding site, and ^{123}FKRRR^{127} bound to the minor binding site, two sodium ions and 79 water molecules. Structural characterization of the interface revealed that PsSiAdV pVII binds to IMPα2 with a canonical monopartite NLS, and a well-characterized lysine at the P2 site (Fig 3b, c). However, a reduced binding interface was resolved in the minor site, a feasible artefact of NLS saturation of the major site (Figs 3b, c and S1).

This binding is typical of a prototypical monopartite NLS, for example SV40 Large T antigen [37], and observed in several other structures [38]. The protein complex was analysed using PDBsum [39] and the interface was found to be mediated by 17 hydrogen bonds and three salt bridges.

PsSiAdV pVII residues 120–128 confer nuclear localization to GFP

Given that PsSiAdV pVII (120–128) can bind to IMPαΔIBB isoforms with high affinity, we decided to investigate its functionality as an IMPα-dependent NLS in a cellular context. To this end, we transiently transfected HEK293A cells to express

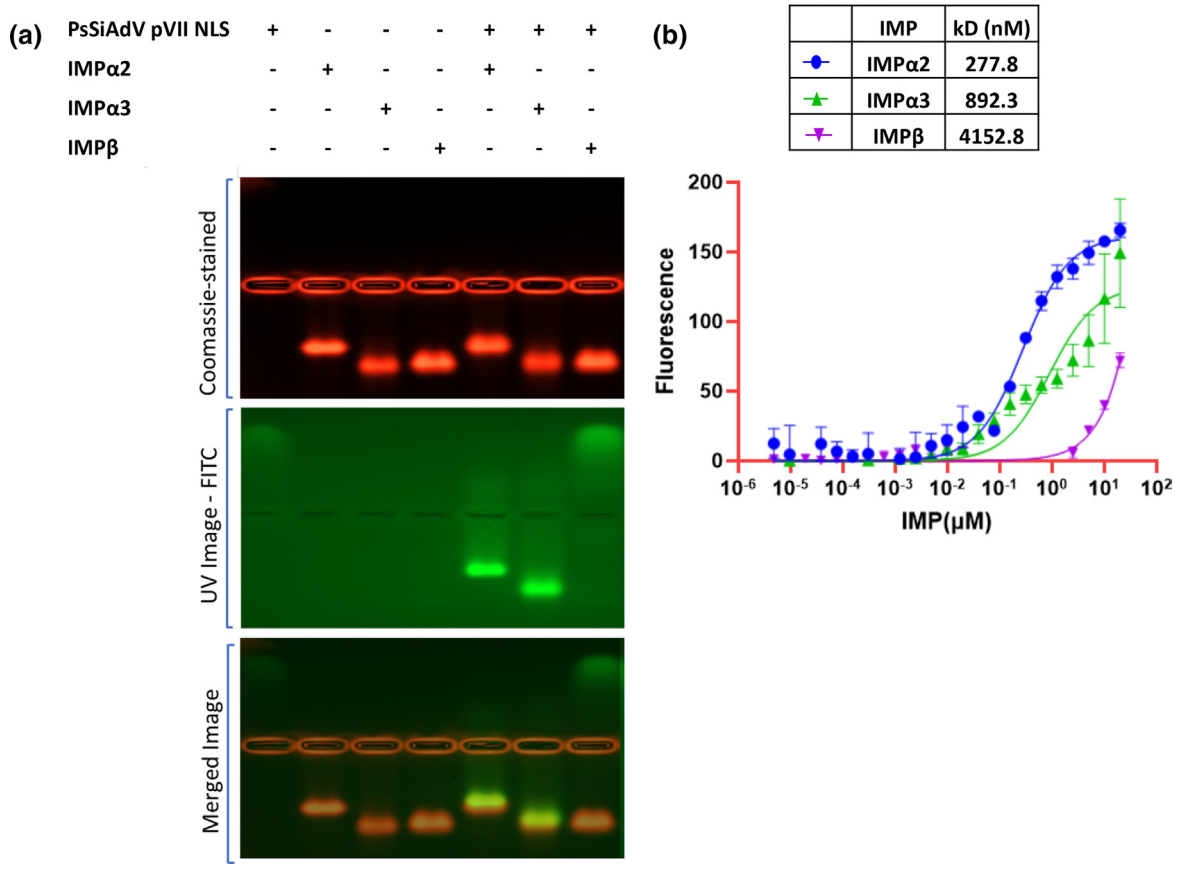

Fig. 2. Binding affinity analysis between the adenovirus pVII-NLS and IMPs. (a) EMSA showing PsSiAdV pVII-NLS binds with ΔIBB-IMPα2 and ΔIBB-IMPα3 isoforms. FITC-tagged PsSiAdV pVII-NLS peptide (residues 120–128) was incubated with IMP isoforms as indicated before electrophoresis and imaging. Coomassie blue-stained protein image (top panel; red) and UV-exposed gel image (middle panel; green) and their overlay (bottom panel) are shown. The yellow colour in the overlay represents the complex formed between IMP and the target peptide. (b) Fluorescence polarization assay measuring the direct binding between PsAdV pVII-NLS and respective IMPα isoforms. Binding interactions were observed across IMPα2 and α3 isoforms where very poor affinity was reflected for IMP*β* at 277.8, 892.3 and 4152.8 nM, respectively. The experiments were conducted in triplicate and error bars represent mean±SEM.

a GFP-PsSiAdV pVII (120–128) fusion protein, in the absence and in the presence of the IMPα/*β* competitive inhibitor Bimax2 [40, 41] fused to mCherry, and quantitatively analysed its level of nuclear accumulation using CLSM at the single-cell level 24 h later. GFP alone and GFP-SV40 LTA cNLS (PKKKRKV-132) were also expressed as negative or positive controls for IMPα/*β*-dependent nuclear accumulation, respectively. As expected, GFP was evenly distributed between the nucleus and cytoplasm, whereas GFP-SV40-LTA cNLS accumulated in the cell nucleus due to its ability to functionally interact with IMPα/*β* (Fig. 4a). Importantly, GFP-PsSiAdV pVII (120–128) similarly accumulated in the cell nucleus, although to lower levels than GFP-SV40-LTA cNLS (Fig. 4b). Quantitative analysis of the Fn/c ratios relative to GFP fusion proteins confirmed that they localized to the cell nucleus to significantly higher levels than GFP alone (Fig. 4c). The highest nuclear targeting activity was measured with SV40 cNLS (Fn/c of 6.6±0.6), followed by PsSiAdV pVII (120–128) (Fn/c of 3.6±0.6). Importantly, co-expression with Bimax2 reduced nuclear localization of GFP-SV40 LTA cNLS and GFP-PsSiAdV pVII (120–128) to levels undistinguishable from those of GFP alone (Fig. 4c). Therefore, PsSiAdV pVII residues 120–128 can be considered a bona fide cNLS.

PsSiAdV pVII protein localizes in the nucleus in the absence of other viral proteins

Since PsSiAdV pVII possesses a bona fide cNLS, we hypothesized it should localize within the cell nucleus, and possibly accumulate into the nucleolus, similarly to its human counterparts. To verify this hypothesis, we compared the subcellular localization of GFP-PsSiAdV and GFP-HAdV-C2 pVII proteins, when expressed in HEK293A cells in the absence of other viral proteins. GFP alone, which equally distributes between the nucleus and cytoplasm, and GFP-UL44, which strongly accumulates within the cell nucleus but not the nucleolus, were also expressed as controls, while DsRed-fibrillarin was used as a marker for nucleoli. Cells were transiently transfected to express the fluorescent fusion proteins (Fig. 5a), and

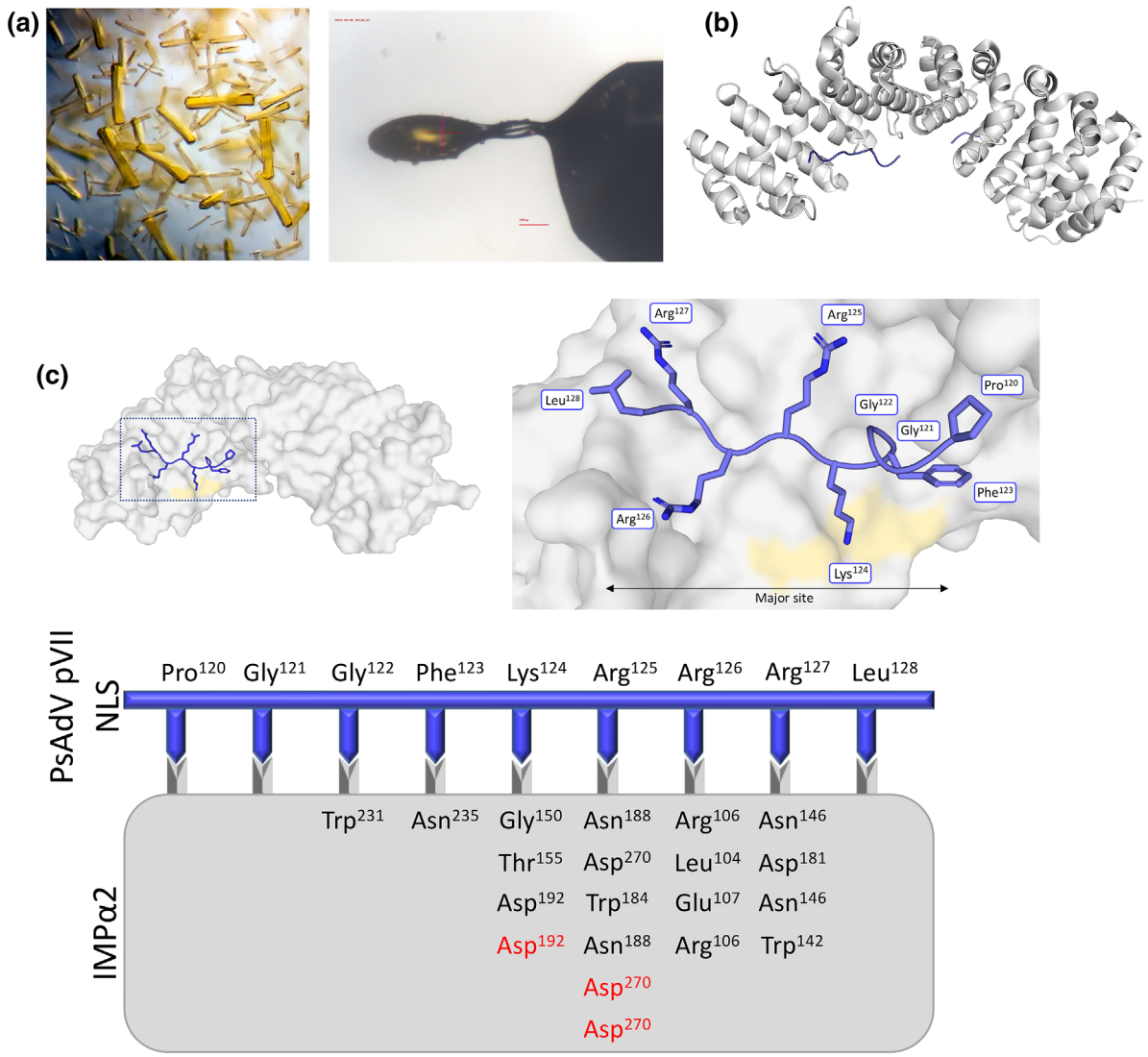

Fig. 3. A schematic illustration of adenovirus PsSiAdV pVII bound to IMPα2. (a) Protein crystals of IMPα2 in complex with PsAdV pVII-NLS. Large rod-shaped crystals were formed after 2 days of incubation at 23°C with 0.6 M sodium citrate, pH 6.5. (b) Structure of IMPα2 (in grey cartoon) with bound PsSiAdV pVII-NLS at the major site (blue stick). (c) The modelled crystal structure of PsSiAdV pVII-NLS bound to IMPα2 was solved to 2.2 Å resolution. IMPα2 (shown in grey surface mode) bound to PsSiAdV pVII-NLS (shown in blue stick mode) at the major binding site. The P2 binding pocket (yellow surface) consists of Gly^{150}, Thr^{155} and Asp^{192}. Images were generated using Pymol software.

their subcellular localization was investigated by CLSM 24 h later. As expected, GFP alone was equally distributed between the nucleus and cytoplasm (Fig. 5b), with an Fn/c of ~1 (Fig. 5c), but was slightly excluded from nucleoli with an Fno/n of ~0.8 (Fig. 5d). On the other hand, GFP-UL44 strongly localized to the cell nucleus, with an Fn/c of 100, but not of nucleoli (Fno/N of ~~0.7), while GFP-HAdV-C2 pVII strongly accumulated into the nucleus (Fn/C ~70), with a clear preference for nucleoli (Fnon 2.2), as previously reported for GFP-HAdV-C5 pre-pVII [7]. Intriguingly, GFP-PsSiAdV pVII accumulated within the cell nucleus (Fn/c of ~40), but was mainly excluded from nucleoli, in contrast to what was previously reported for GFP- HAdV-C5 (Fno/n 0.8; Fig. 5d)

PsSiAdV pVII protein can accumulate in the nucleus independently of the IMPα/β heterodimer

We then analysed the subcellular localization of pVII when expressed in the presence or absence of DsRed-RanQ69L, a Ran dominant negative mutant with impaired GTPase activity capable of inhibiting IMP-mediated nuclear transport, as well as mCherry-Bimax2 as performed above (Fig. 6). GFP-HCMV UL44 was also expressed as a control. As expected, upon co-expression with either DsRed-RanQ69L or mCherry-Bimax2, the nuclear accumulation of GFP-HCMV UL44 was significantly impaired (Fig. 6b–d). Expression of DsRed-RanQ69L did not prevent nuclear localization of GFP-PsSiAdV

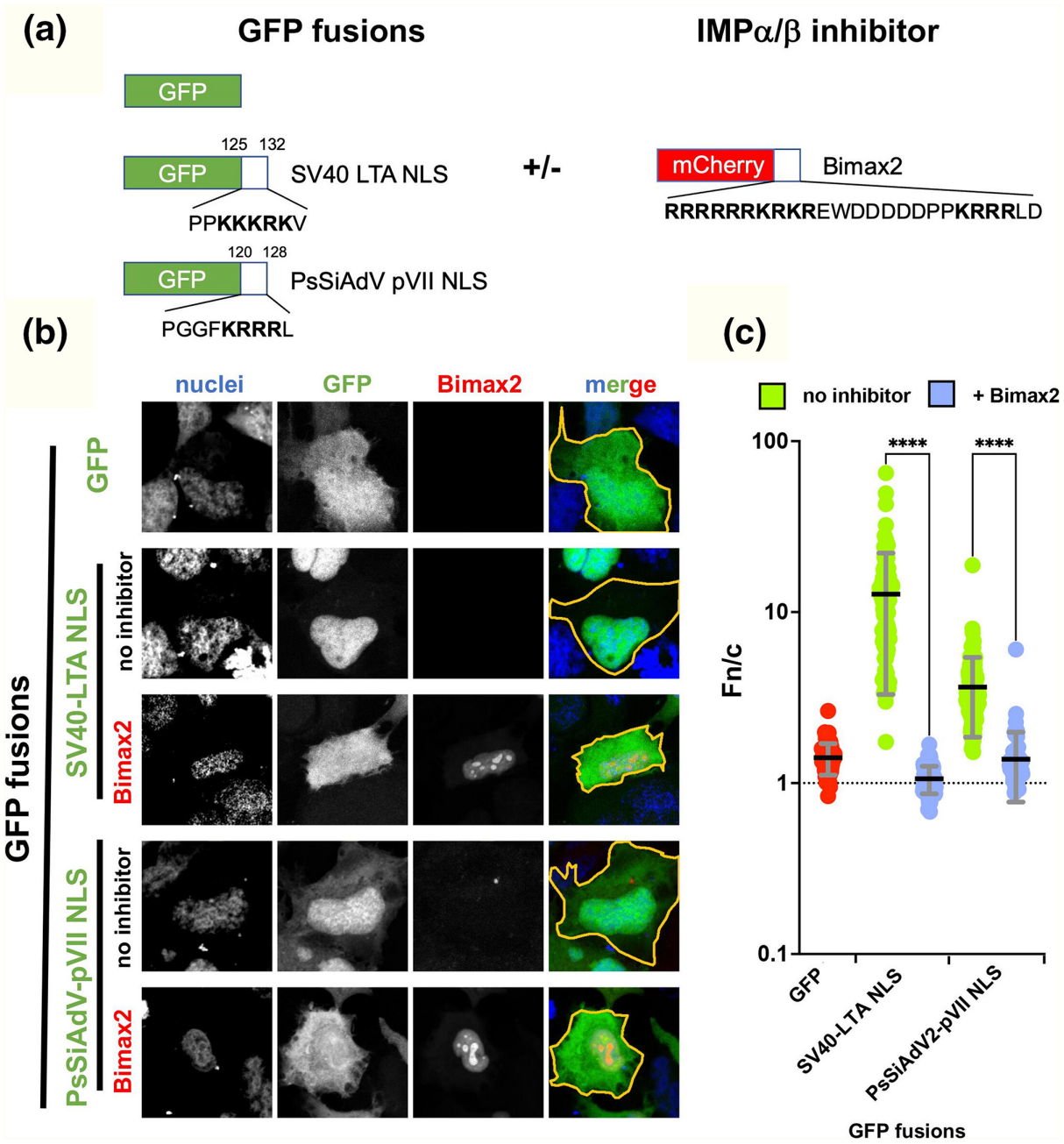

Fig. 4. PsSiAdV pVII residues 120–128 confer IMPα/β-dependent nuclear targeting to GFP. (a) HEK293A cells were transfected to express the indicated GFP fusion proteins, in the presence or absence of the IMPα/β nuclear import mcherry-Bimax2. (b) At 24 h post-transfection cells were incubated with DRAQ5 to stain cell nuclei, then fixed, and coverslips were mounted on slide holders before being analysed by using a Nikon A1 CLSM equipped with a 60× oil immersion objective. The 633 nm (nuclei), 488 nm (GFP) and 561 nm (Bimax2) channels are shown, along with a merged image (merge), whereby the cell boundaries of analysed cells are coloured in orange. (c) Micrographs such as those shown in (b) were quantitatively analysed to calculate the levels of nuclear accumulation (Fn/c) relative to the indicated fusion proteins at the single-cell level, as described in the Methods. Data shown are individual measurements with mean±SD relative to pooled data from at least 72 cells and two independent experiments. Results from an ordinary one-way ANOVA test for the nuclear accumulation of the indicated GFP-fusion proteins are expressed alone or in the presence of mCherry-Bimax2. ****P<0.0001.

pVII (Fig. 6b). However, its levels of nuclear accumulation were reduced by ~50%, with a reduction of the Fn/c value from 40 to ~20 (Fig. 6c). Indeed, we measured a decrease in the percentage of cells whereby GFP-PsSiAdV pVII strongly accumulated in the cell nucleus (Fn/c>10; from 93 to 83%; Fig. 6c). This is probably the consequence of PsSiAdV pVII being able to passively diffuse into the cell nucleus due to its low molecular weight, and potentially to use multiple nuclear import

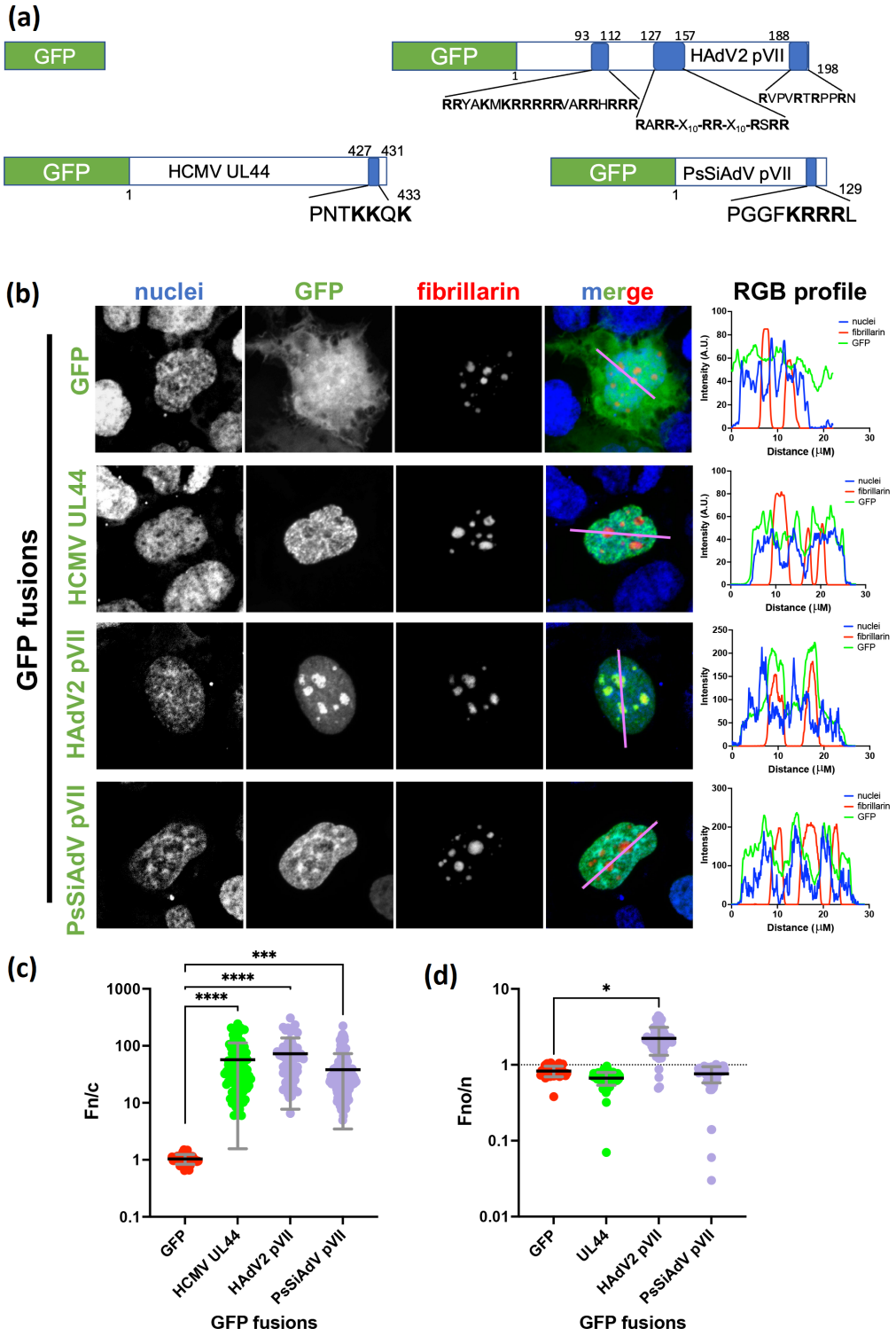

Fig. 5. PsSiAdV pVII protein accumulates in the nucleus but not in the nucleolus when expressed in the absence of additional viral proteins. (a) HEK293A cells were transfected to express the indicated GFP fusion proteins, in the presence or absence of the nucleolus marker DsRed-fibrillarin. NLSs are represented as blue vertical boxes, and their sequence is indicated with the single letter amino acid code and basic residues in bold type. (b) At 24 h post-transfection cells were incubated with DRAQ5 to stain cell nuclei, then fixed, and coverslips were mounted on slide holders before being analysed by using a Nikon A1 CLSM device equipped with a 60× oil immersion objective. The 633 nm (nuclei), 488 nm (GFP) and 561 nm (fibrillarin) channels are shown, along with a merged image (merge), and an RGB plot profile of the region of interest highlighted in the merged image. Micrographs such as those shown in (b) were quantitatively analysed to calculate the levels of nuclear (c) and nucleolar (d) accumulation relative to the indicated fusion proteins at the single-cell level. Data shown are individual measurements with mean±SD relative to pooled data from at least 58 cells and three independent experiments. Results from the ordinary one-way ANOVA test for the nuclear accumulation of the indicated GFP-fusion proteins as compared to GFP alone are shown. *P<0.05; ***P<0.001; ****P<0.0001.

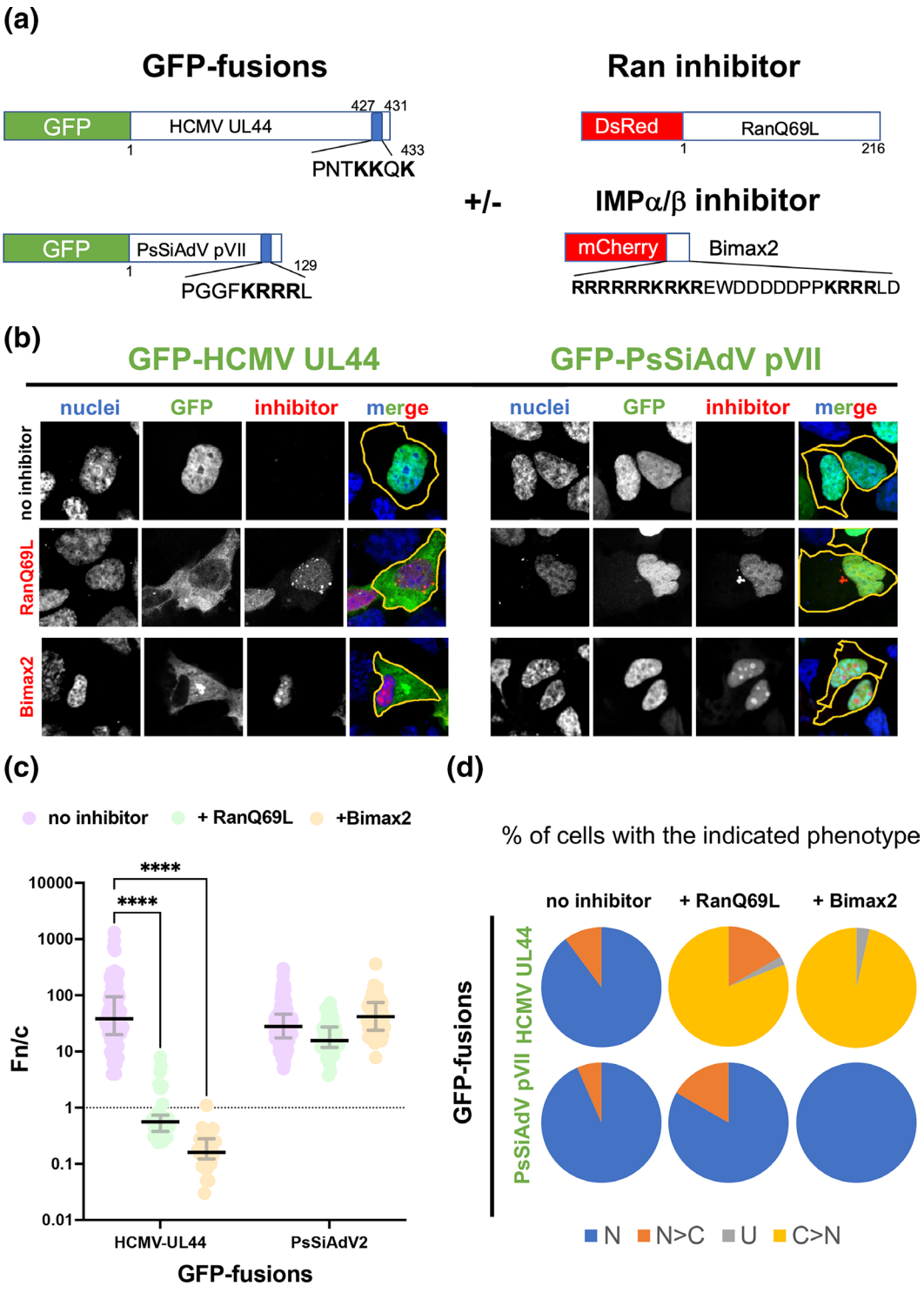

Fig. 6. PsSiAdV pVII can be imported into the nucleus via IMPα/*β*-independent pathways. (a) The indicated GFP fusion proteins were transiently expressed in HEK293A, in the absence or presence of either the Ran-dependent nuclear import inhibitor DsRed-RanQ69L or the IMPα/*β*-dependent nuclear import inhibitor mCherry-Bimax2. (b) At 24 h post-transfection cells were incubated with DRAQ5 to stain cell nuclei, then fixed, and coverslips were mounted on slide holders before being analysed by using a Nikon A1 CLSM device equipped with a 60× oil immersion objective. The 633 nm (nuclei), 488 nm (GFP) and 561 nm (Bimax2) channels are shown, along with a merged image (merge), whereby the cell boundaries of analysed cells are coloured in orange. (c) Micrographs such as those shown in (b) were quantitatively analysed to calculate the levels of nuclear accumulation (Fn/c) relative to the indicated fusion proteins at the single-cell level. Data shown are individual measurements with mean±SD relative to pooled data from at least 28 cells and two independent experiments. Results from two-way ANOVA tests for the nuclear accumulation of the indicated GFP-fusion proteins in the absence or presence of RanQ69L/Bimax2 are shown. ****P<0.0001. The subcellular localization of the indicated GFP fusion protein at the single-cell level was classified as nuclear (N: Fn/c>10), more nuclear than cytosolic (N>C: 2<Fn/c<10), ubiquitous (U: 1<Fn/c<2) or more cytosolic than nuclear (C>N: Fn/c<1). The percentage of cells with the indicated phenotypes is shown.

pathways. Surprisingly, nuclear accumulation of GFP-PsSiAdV pVII was not affected by co-expression with mCherry-Bimax2 (Fig. 6b–d). Our results suggest that, in addition to being able to passively diffuse in the cell nucleus and to be actively transported in the cell nucleus by the IMPα/*β* heterodimer through recognition of the cNLS located at residues 120–128, PsSiAdV pVII is also imported via multiple IMPα-independent mechanisms similarly to what has been reported for the pVII of HAdV [6–8].

DISCUSSION

Adenoviruses are DNA viruses that are known to replicate within the cell nucleus [42, 43] and knowledge of the behaviour and localization of viral proteins are important to understanding viral replication and thereby to developing antiviral strategies. Adenoviruses use multiple nuclear localization mechanisms during infection [8], and the core protein pVII has been shown to play a crucial role in regulating nuclear trafficking [3, 6, 8]. However, the exact mechanism is not well understood. Therefore, to further investigate this we employed a combination of structural, biophysical and cellular data analysis to study the function of classical NLSs in PsSiAdV pVII and their interaction with cellular IMPs.

HAdV was previously reported to have multiple NLS regions: classical, non-classical and bipartite NLSs [6–8]. The study of HAdV-C by Lee *et al*. [7] and Wodrich *et al*. [8] observed karyophilic activity in both the C- and N-terminal NLSs with differential preference for IMPs. The family *Adenoviridae* exhibits substantial diversity in genome size and gene content. The recently discovered psittacine siadenovirus F is of particular significance as it causes diseases among the critically endangered Australian parrot, the orange-bellied parrot [1]. There is a pressing need for a better understanding of psittacine adenovirus F to develop therapeutic options. Here we studied a predicted cNLS region in PsSiAdV pVII at the C-terminus spanning amino acids 120–128. Amino acid sequences of NLS regions in PsSiAdV and HAdV-C are not conserved (Fig. 1), which could be a result of variations in genome size and pVII gene length (25.3 kb and 128 aa for PsSiAdV; 35.9 kb and 198 aa for HAdV-C2). However, as expected, the GFP-PsSiAdV pVII-cNLS fusion protein was localized within the cell nucleus (Fig. 4), confirming the capacity of this sequence to promote nuclear import.

The ability of NLSs of pVII to recognize and bind multiple import receptors has been demonstrated previously [8]. Biochemical analysis also showed the co-migration of FITC-labelled peptide with IMPα2 and α3 with polarization assays demonstrating high affinity for IMPα2ΔIBB and IMPα3ΔIBB. This study further resolves the high-resolution crystal structure of the binding interface between IMPα2ΔIBB and PsSiAdV pVII-NLS, demonstrating strong affinity. PsSiAdV pVII-NLS was found to bind at both the major and the minor sites with the major binding site interaction demonstrating the classic lysine residue at the conserved P2 site in IMPα2. In contrast, both FP and EMSA assays showed that IMP*β* did not bind PsSiAdV pVII-NLS (120–128) which suggests that direct interaction with IMP*β* is not involved in the transport of this NLS into the cell nucleus [44]. Differential import preference has been previously observed in studies on HAdV pVII. Wodrich, *et al*. [8] demonstrated that HAdV-C5 pre-pVII interacts with multiple IMPs including IMP*β* while Hindly *et al*. [6] reported that pre-VII and mature VII preferentially bind IMPα and transportin respectively.

Our investigation to determine the subcellular distribution of PsSiAdV pVII showed specific accumulation within the cell nucleus. However, unlike pVII from HAdV-C2 (Fig. 5) and HAdV-C5 [7] which accumulated in the nucleolus, PsSiAdV pVII was mainly nucleoplasmic and partly excluded from the nucleoli. The nucleolus is the most prominent nuclear domain and some virally induced modifications in the nucleolus are involved in regulating processes such as cell cycle, cell stress responses and protein translation that are crucial for the outcome of infection [45, 46]. HAdV has previously been reported to contain arginine-rich nucleolar targeting sequences and it has been hypothesized that the charge-to-mass ratio might be responsible for nucleolar targeting [7]. It is also possible that the cellular distribution of viral DNA can be influenced by the host species and host environmental factors [47] which might be the reason for the exclusion of nucleolar translocation shown in this study, but this requires further evaluation.

To determine whether the nuclear targeting is due to IMPα/*β* active transport, the IMPα competitive inhibitor Bimax2 and a RanQ69L, which is capable of inhibiting IMP-mediated nuclear transport, were co-expressed with GFP-PsSiAdV pVII but neither inhibitor prevented the nuclear transport of PsSiAdV pVII. PsSiAdV may possess distinctive transport mechanisms to bypass the dependency on specific import proteins. Instead of relying on IMP-mediated transport alone, PsSiAdV pVII may directly interact with components of the nuclear pore complex enabling the nuclear import of viral DNA as seen in other adenoviral proteins [5, 42]. For instance, hexon, the major capsid protein, was found to form a direct interaction with the nuclear pore complex during the nuclear import of DNA [42]. A study by Dai *et al*. [5] demonstrated the binding interface between the cleaved N-terminus of pre-pVII and hexon, providing evidence for the utilization of genome–capsid co-assembly mechanisms used in adenoviruses during nuclear import. However, these hypotheses require further investigation for confirmation.

Overall, our results suggest that the predicted C-terminal NLS in PsSiAdV pVII is involved in IMPα-mediated nuclear transport of PsSiAdV but there is also the possibility for nuclear localization through alternative transport mechanisms

other than the IMPα/*β* active transport. It is likely that species-specific and multiple transport mechanisms are involved during adenovirus nuclear localization. However, we employed a human cell line for our subcellular localization experiments. Therefore, to obtain a clear understanding of this process, further investigations into other potential nuclear localization sequences are recommended. Additionally, while this study focused on PsSiAdV pVII, it would be valuable to examine whether similar mechanisms exist in other adenoviruses by comparing the behaviour of pVII across different adenovirus species. Taken together, these studies on adenovirus pVII are significant for advancing our understanding of adenovirus biology, facilitating the development of antiviral therapies and vaccines, and contributing to the broader field of virology.

Funding information
Subir Sarker is the recipient of an Australian Research Council Discovery Early Career Researcher Award (grant number DE200100367) funded by the Australian Government. Ajani Athukorala is supported by the La Trobe University (LTU) under the LTU Graduate Research Scholarship and LTU Full Fee Research Scholarship. The funders had no role in the design of the study; in the collection, analyses, or interpretation of data; in the writing of the manuscript, or in the decision to publish the results.

Author contributions
Conceptualization was done by A.A., B.P.M., J.K.F., G.A., S.S., experiments were performed by A.A., S.P., S.N., V.A.D., B.N., data acquisition and analysis by A.A., C.M.D., G.A., S.N., writing of initial draft by A.A., review and editing by A.A., C.M.D., S.P., S.N., V.A.D, B.N., K.J.H., B.P.M., G.A., J.K.F., S.S., E.D., and supervision and funding acquisition by S.S. All authors have read and agreed to the published version of the manuscript.

Conflicts of interest
All authors declare that they have no conflicts of interest.

References

1. Athukorala A, Helbig KJ, Mcsharry BP, Forwood JK, Sarker S. Adenoviruses in avian hosts: recent discoveries shed new light on adenovirus diversity and evolution. *Viruses* 2022;14:1767.
2. Gallardo J, Pérez-Illana M, Martín-González N, San Martín C. Adenovirus structure: what is new? *Int J Mol Sci* 2021;22:5240.
3. Kulanayake S, Tikoo SK. Adenovirus core proteins: structure and function. *Viruses* 2021;13:388.
4. Benkő M, Aoki K, Arnberg N, Davison AJ, Echavarría M, *et al*. ICTV Virus Taxonomy Profile: *Adenoviridae* 2022. *J Gen Virol* 2021;103.
5. Dai X, Wu L, Sun R, Zhou ZH, Banks L. Atomic structures of minor proteins VI and VII in human adenovirus. *J Virol* 2017;91:e00850-17.
6. Hindley CE, Lawrence FJ, Matthews DA. A role for transportin in the nuclear import of adenovirus core proteins and DNA. *Traffic* 2007;8:1313–1322.
7. Lee TWR, Blair GE, Matthews DA. Adenovirus core protein VII contains distinct sequences that mediate targeting to the nucleus and nucleolus, and colocalization with human chromosomes. *J Gen Virol* 2003;84:3423–3428.
8. Wodrich H, Cassany A, D'Angelo MA, Guan T, Nemerow G, *et al*. Adenovirus core protein pVII is translocated into the nucleus by multiple import receptor pathways. *J Virol* 2006;80:9608–9618.
9. Avgousti DC, Herrmann C, Kulej K, Pancholi NJ, Sekulic N, *et al*. A core viral protein binds host nucleosomes to sequester immune danger signals. *Nature* 2016;535:173–177.
10. Avgousti DC, Della Fera AN, Otter CJ, Herrmann C, Pancholi NJ, *et al*. pVII downregulates the DNA damage response. *J Virol* 2017;91:e01089-17.
11. Inturi R, Mun K, Singethan K, Schreiner S, Pungaa T. Human adenovirus infection causes cellular E3 ubiquitin ligase MKRN1 degradation involving the viral core protein pVII. *J Virol* 2017;92:e01154-17.
12. Karen KA, Hearing P. Adenovirus core protein VII protects the viral genome from a DNA damage response at early times after infection. *J Virol* 2011;85:4135–4142.
13. Lu J, Wu T, Zhang B, Liu S, Song W, *et al*. Types of nuclear localization signals and mechanisms of protein import into the nucleus. *Cell Commun Signal* 2021;19:60.
14. Jäkel S, Mingot J-M, Schwarzmaier P, Hartmann E, Görlich D. Importins fulfil a dual function as nuclear import receptors and cytoplasmic chaperones for exposed basic domains. *EMBO J* 2002;21:377–386.
15. Athukorala A, Phalen DN, Das A, Helbig KJ, Forwood JK, *et al*. Genomic characterisation of a highly divergent Siadenovirus (Psittacine Siadenovirus F) from the critically endangered orange-bellied parrot (*Neophema chrysogaster*). *Viruses* 2021;13:1714.
16. Kosugi S, Hasebe M, Tomita M, Yanagawa H. Systematic identification of cell cycle-dependent yeast nucleocytoplasmic shuttling proteins by prediction of composite motifs. *Proc Natl Acad Sci U S A* 2009;106:10171–10176.
17. Munasinghe TS, Edwards MR, Tsimbalyuk S, Vogel OA, Smith KM, *et al*. MERS-CoV ORF4b employs an unusual binding mechanism to target IMPα and block innate immunity. *Nat Commun* 2022;13:1604.
18. Teh T, Tiganis T, Kobe B. Crystallization of importin alpha, the nuclear-import receptor. *Acta Crystallogr D Biol Crystallogr* 1999;55:561–563.
19. Studier FW. Protein production by auto-induction in high density shaking cultures. *Protein Expr Purif* 2005;41:207–234.
20. Aragão D, Aishima J, Cherukuvada H, Clarken R, Clift M, *et al*. MX2: a high-flux undulator microfocus beamline serving both the chemical and macromolecular crystallography communities at the Australian Synchrotron. *J Synchrotron Radiat* 2018;25:885–891.
21. Battye TGG, Kontogiannis L, Johnson O, Powell HR, Leslie AGW. iMOSFLM: a new graphical interface for diffraction-image processing with MOSFLM. *Acta Crystallogr D Biol Crystallogr* 2011;67:271–281.
22. Evans PR. An introduction to data reduction: space-group determination, scaling and intensity statistics. *Acta Crystallogr D Biol Crystallogr* 2011;67:282–292.
23. Emsley P, Lohkamp B, Scott WG, Cowtan K. Features and development of Coot. *Acta Crystallogr D Biol Crystallogr* 2010;66:486–501.
24. Adams PD, Afonine PV, Bunkóczi G, Chen VB, Davis IW, *et al*. PHENIX: a comprehensive Python-based system for macromolecular structure solution. *Acta Crystallogr D Biol Crystallogr* 2010;66:213–221.
25. McCoy AJ, Grosse-Kunstleve RW, Adams PD, Winn MD, Storoni LC, *et al*. Phaser crystallographic software. *J Appl Crystallogr* 2007;40:658–674.
26. Alvisi G, Manaresi E, Cross EM, Hoad M, Akbari N, *et al*. Importin α/*β*-dependent nuclear transport of human parvovirus B19 nonstructural protein 1 is essential for viral replication. *Antiviral Res* 2023;213:105588.
27. Alvisi G, Jans DA, Guo J, Pinna LA, Ripalti A. A protein kinase CK2 site flanking the nuclear targeting signal enhances nuclear transport of human cytomegalovirus ppUL44. *Traffic* 2005;6:1002–1013.
28. Alvisi G, Jans DA, Ripalti A. Human cytomegalovirus (HCMV) DNA polymerase processivity factor ppUL44 dimerizes in

the cytosol before translocation to the nucleus. *Biochemistry* 2006;45:6866–6872.

29. Alvisi G, Avanzi S, Musiani D, Camozzi D, Leoni V, *et al*. Nuclear import of HSV-1 DNA polymerase processivity factor UL42 is mediated by a C-terminally located bipartite nuclear localization signal. *Biochemistry* 2008;47:13764–13777.
30. Heilman DW, Teodoro JG, Green MR. Apoptin nucleocytoplasmic shuttling is required for cell type-specific localization, apoptosis, and recruitment of the anaphase-promoting complex/cyclosome to PML bodies. *J Virol* 2006;80:7535–7545.
31. Tsujii A, Miyamoto Y, Moriyama T, Tsuchiya Y, Obuse C, *et al*. Retinoblastoma-binding protein 4-regulated classical nuclear transport is involved in cellular senescence. *J Biol Chem* 2015;290:29375–29388.
32. Gomez Corredor A, Archambault D. The bovine immunodeficiency virus rev protein: identification of a novel lentiviral bipartite nuclear localization signal harboring an atypical spacer sequence. *J Virol* 2009;83:12842–12853.
33. Smith KM, Di Antonio V, Bellucci L, Thomas DR, Caporuscio F, *et al*. Contribution of the residue at position 4 within classical nuclear localization signals to modulating interaction with importins and nuclear targeting. *Biochim Biophys Acta* 2018;1865:1114–1129.
34. Di Antonio V, Palù G, Alvisi G. Live-cell analysis of human cytomegalovirus DNA polymerase holoenzyme assembly by resonance energy transfer methods. *Microorganisms* 2021;9:928.
35. Alvisi G, Paolini L, Contarini A, Zambarda C, Di Antonio V, *et al*. Intersectin goes nuclear: secret life of an endocytic protein. *Biochem J* 2018;475:1455–1472.
36. Trevisan M, Di Antonio V, Radeghieri A, Palù G, Ghildyal R, *et al*. Molecular requirements for self-interaction of the respiratory syncytial virus matrix protein in living mammalian cells. *Viruses* 2018;10:109.
37. Fontes MRM, Teh T, Kobe B. Structural basis of recognition of monopartite and bipartite nuclear localization sequences by mammalian importin-α11Edited by K. Nagai. *J Mol Biol* 2000;297:1183–1194.
38. Oka M, Yoneda Y. Importin α: functions as a nuclear transport factor and beyond. *Proc Jpn Acad Ser B Phys Biol Sci* 2018;94:259–274.
39. Laskowski RA, Jabłońska J, Pravda L, Vařeková RS, Thornton JM. PDBsum: structural summaries of PDB entries. *Protein Sci* 2018;27:129–134.
40. Kosugi S, Hasebe M, Entani T, Takayama S, Tomita M, *et al*. Design of peptide inhibitors for the importin α/β nuclear import pathway by activity-based profiling. *Chem Bioi* 2008;15:940–949.
41. Mehmood R, Yasuhara N, Fukumoto M, Oe S, Tachibana T, *et al*. Cross-talk between distinct nuclear import pathways enables efficient nuclear import of E47 in conjunction with its partner transcription factors. *Mol Biol Cell* 2011;22:3715–3724.
42. Cassany A, Ragues J, Guan T, Bégu D, Wodrich H, *et al*. Nuclear import of Adenovirus DNA involves direct interaction of hexon with an N-Terminal domain of the nucleoporin Nup214. *J Virol* 2015;89:1719–1730.
43. Fay N, Panté N. Nuclear entry of DNA viruses. *Front Microbiol* 2015;6:467.
44. Wagstaff KM, Dias MM, Alvisi G, Jans DA. Quantitative analysis of protein-protein interactions by native page/fluorimaging. *J Fluoresc* 2005;15:469–473.
45. Hiscox JA, Whitehouse A, Matthews DA. Nucleolar proteomics and viral infection. *Proteomics* 2010;10:4077–4086.
46. Salvetti A, Greco A. Viruses and the nucleolus: the fatal attraction. *Biochim Biophys Acta* 2014;1842:840–847.
47. Flatt JW, Butcher SJ. Adenovirus flow in host cell networks. *Open Biol* 2019;9:190012.